

An investigation into the asymptotics of the meromorphic 3D-index.

Andrew Kricker

Nanyang Technological University, Singapore

1 Introduction

This article will describe some of the investigations that led to the work “On the asymptotics of the meromorphic 3D-index”, which is joint work with Craig Hodgson and Rafael Siejakowski [1].

There are two types of “3D-index” in this story: the q -series 3D-index, and the meromorphic 3D-index. Our focus was on the meromorphic 3D-index, and in particular its asymptotic properties.

The original version of the 3D-index is the **q -series 3D-index** introduced by Dimofte, Gaiotto, and Gukov [3, 4]. They discovered this construction in the theoretical physics context of supersymmetric gauge field theories. The mathematical definition was clarified and studied first by Garoufalidis [5]. The construction is defined on (a suitable) ideal triangulation \mathcal{T} of a connected oriented 3-manifold M with boundary k torus components, and yields a function which associates a Laurent series in the formal parameter $q^{1/2}$ to each class in H_1 of the boundary.

$$I_{\mathcal{T}} : H_1(\partial M, \mathbb{Z}) \rightarrow \mathbb{Z}((q^{1/2})).$$

This construction converges precisely for triangulations which are 1-efficient [7]. So even though it is invariant under 2-3 Pachner moves in the case the invariant is defined on both sides of the move, it does not follow that it is a topological invariant. [7] nevertheless found a way to use the known properties to get a genuine topological invariant in the case the manifold is complete hyperbolic, using special facts true in this case. It is worth noting that the theoretical physics theory this invariant arises from predicts that it is in fact a genuine topological invariant.

[6] interpreted the invariant as a certain sum over normal surfaces with specified boundary.

The second version of 3D-index is the **meromorphic 3D-index**. This was introduced in 2019 by Garoufalidis and Kashaev [8]. Their construction associates a complex meromorphic function of $2k$ variables to a triangulation with k torus boundary components.

From here on we’ll specialize the discussion to the case $k = 1$. The choice of the 2 variables e_{μ} and e_{λ} of the meromorphic function in this case correspond to a choice of simple closed curves μ and λ representing a basis of H_1 . We’ll discuss some details of this later in this article.

The meromorphic 3D-index improves on the q -series 3D-index in that Garoufalidis and Kashaev define it on every triangulation, and argue the resulting meromorphic function is invariant under all Pachner moves [8]. Because they show the meromorphic 3D-index is in fact a topological invariant, we can write it as a function of M , not just the triangulation \mathcal{T} :

$$I_{M,q}(e_\mu, e_\lambda).$$

Garoufalidis and Kashaev show that the two versions of 3D-index are related for triangulations which admit a *strict angle structure* [8]. A strict angle structure is an assignment of strictly positive reals to each quad type of the triangulation (a quad type is a pair of opposite edges in a tetrahedron) such that the 3 assignments to each tetrahedra add up to π , and such that the assignments around each edge of the triangulation add up to 2π . We denote a strict angle structure $\alpha: Q(\mathcal{T}) \rightarrow \mathbb{R}_{>0}$. For example a triangulation admitting a positively oriented solution of Thurston's gluing equations admits a strict angle structure. For triangulations admitting a strict angle structure there is a proof in [8] that

$$I_{M,q}(e_\mu, e_\lambda) = \sum_{a,b \in \mathbb{Z}} e_\mu^a e_\lambda^b I_{\mathcal{T}}(a[\lambda] - b[\mu]) (q^2).$$

Thus we can think of the q -series 3D-index as a kind of “Fourier transform” of the meromorphic 3D-index.

This formula establishes that the q -series 3D-index is in fact a topological invariant of 3-manifolds admitting an ideal triangulation carrying a strict angle structure. Any choice of triangulation carrying a strict angle structure should yield the same q -series 3D-index.

2 What is the meaning of the variables e_μ and e_λ of the meromorphic function $I_{M,q}(e_\mu, e_\lambda)$?

The meromorphic 3D-index was defined in [8] by means of a “state-integral”. The states being integrated over are an assignment of a complex number of modulus 1 to each edge of the triangulation. This GK state-integral expression depends on the ideal triangulation \mathcal{T} and also a strict angle structure α on it. The space of strict angle structures on \mathcal{T} is a convex subset of \mathbb{R}^{n+1} where n is the number of tetrahedra in the triangulation.

But it turns out that the GK state-integral only depends on the space of strict angle structures through two linear functions on the space: the *peripheral angle holonomies* [8]. Let's briefly define these quantities.

Let α be a strict angle structure on \mathcal{T} and let γ be an oriented simple closed curve on the triangulation of the boundary torus induced from the ideal triangulation \mathcal{T} . Assume γ is in normal position with respect to that triangulation. The angle holonomy of γ with respect to α is the signed sum of the angles associated by α to vertices of triangles cut-off by γ . If γ goes around a vertex in counter-clockwise fashion the angle contributes with a plus sign. If it goes around the vertex in clockwise fashion then it contributes with a minus sign. It turns out this quantity only depends on the choice of simple closed curve up to isotopy.

Let μ and λ denote two such simple closed curves whose corresponding homology classes give a basis for the first homology of the boundary. Garoufalidis and Kashaev show that

their state-integral factors through the corresponding peripheral angle holonomies A_μ and A_λ . The variables e_μ and e_λ are determined from these by the expressions

$$e_\mu = (-q)^{A_\mu/\pi}, \quad e_\lambda = (-q)^{A_\lambda/2\pi}.$$

Thus the meromorphic function $I_{M,q}(e_\mu, e_\lambda)$ is defined by the commutative diagram:

$$\begin{array}{ccc} \{\text{Strict angle structures on } \mathcal{T}\} & \xrightarrow{\text{GK state integral}} & \mathbb{C} \\ \downarrow \text{Peripheral angle holonomies } (A_\mu, A_\lambda) & \searrow I_{M,q}((-q)^{A_\mu/\pi}, (-q)^{A_\lambda/2\pi}) & \\ \mathbb{C}^2 & & \end{array}$$

Strictly speaking: the peripheral angle holonomies are real quantities. The GK state integral defines the germ of an analytic function on a real hyperplane in \mathbb{C}^2 , and the meromorphic function is defined by analytic continuation from that [8].

3 Our study: The case of 1-cusped hyperbolic manifolds.

Our investigation [1] considered the case when the ideal triangulation is equipped with a positively oriented solution $z: Q(\mathcal{T}) \rightarrow \mathbb{C}$ to Thurston's gluing and completeness equations. This solution equips M with a unique complete hyperbolic structure.

In this case the principal argument of the solution z gives a strict angle structure on \mathcal{T} with vanishing peripheral angle holonomy: $A_\mu = A_\lambda = 0$.

The GK state integral evaluated with respect to this special angle structure computes the value of the meromorphic function at the canonical point $(1, 1)$.

Our focus was the asymptotic behaviour of this value as the quantum parameter q approached 1^- . So we set $q = e^{-\kappa}$ and studied

$$I_{M,e^{-1/\kappa}}(1, 1), \quad \text{as } \kappa \rightarrow \infty.$$

4 Numerical experiments and our resulting hypotheses.

Our collaboration began by independently preparing several different computer programs to investigate the behaviour of this value $I_{M,e^{-1/\kappa}}(1, 1)$ in the direction $\kappa \rightarrow \infty$. Results of the different computational approaches we tried were verified against each other.

As we performed experiments we developed hypotheses about what form the leading asymptotics took. The picture we developed through this process was that the leading asymptotics of $I_{M,e^{-1/\kappa}}(1, 1)$ should consist of a sum over certain boundary-parabolic representations $\rho: \pi_1(M) \rightarrow PSL(2, \mathbb{C})$, where the terms of the sum depended in an explicit way on topological and geometric information associated to the representations.

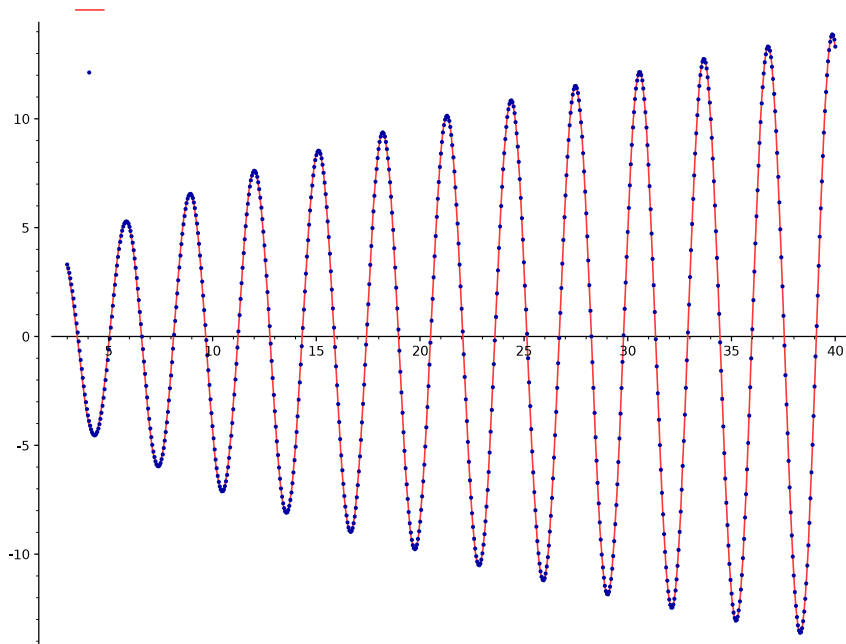


Figure 1: The case of the manifold $M = S^3 \setminus 4_1$, which is the complement of the figure-of-8 knot. The red dots show our numerical computation of $I_{M, e^{-1/\kappa}}(1, 1)$ for $\kappa = 3, 3.1, 3.2, \dots, 39.9, 40$. The curve shown fit to these points is $\frac{2\sqrt{2\pi}}{\sqrt[4]{27}} \sqrt{\kappa} \cos(2.030\kappa + \frac{\pi}{4})$.

4.1 The case $M = S^3 \setminus 4_1$.

The first manifold we studied was $M = S^3 \setminus 4_1$, the figure-of-8 knot complement, which has a classic 2 ideal tetrahedra triangulation. The results of the computation are shown in Figure 1. We found that the data points are tightly fit by the following function:

$$\frac{2\sqrt{2\pi}}{\sqrt[4]{27}} \sqrt{\kappa} \cos\left(2.030\kappa + \frac{\pi}{4}\right).$$

This led to our first experimental discovery: the frequency of the cos factor is approximately the hyperbolic volume of M :

$$\text{Vol}_{\mathbb{H}}(M) \approx 2.030.$$

4.2 The case $M = S^3 \setminus 5_2$.

The next manifold we studied was the complement of the knot 5_2 , which has a 3 ideal tetrahedron triangulation. The results of this experiment are shown in Figure 2.

In this example as well, the volume appeared as the frequency of a trigonometric contribution. Indeed the computations are well fit by the following expression, where $\text{Vol}_{\mathbb{H}}(S^3 \setminus 5_2)$ denotes the hyperbolic volume of the space:

$$0.534\kappa + 1.769\sqrt{\kappa} \cos\left(\kappa \text{Vol}_{\mathbb{H}}(S^3 \setminus 5_2) + \frac{\pi}{4}\right).$$

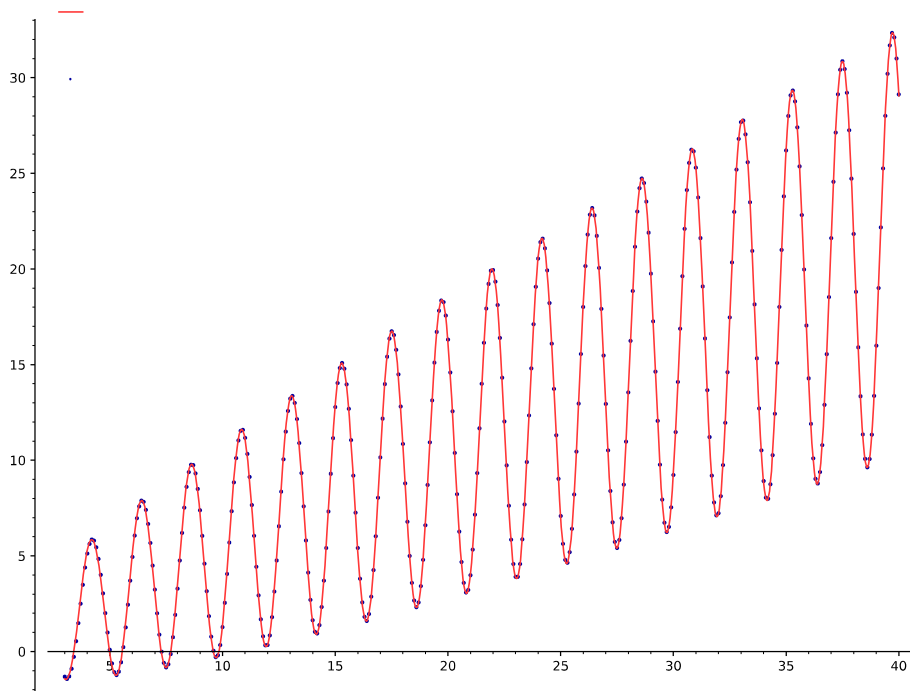


Figure 2: The case of the manifold $M = S^3 \setminus 5_2$. The curve shown fit to the computations is $0.534\kappa + 1.769\sqrt{\kappa} \cos(\kappa \text{Vol}_{\mathbb{H}}(S^3 \setminus 5_2) + \frac{\pi}{4})$.

But this expression contains a surprise, compared to the case of 4_1 . There also appeared to be a linear term! Namely, 0.534κ .

We eventually understood, as we discuss below, that this example has a **real** boundary-parabolic representation $\rho: \pi_1(S^3 \setminus 5_2) \rightarrow PSL(2, \mathbb{R}) \subset PSL(2, \mathbb{C})$. On the other hand, $S^3 \setminus 4_1$ does not, so there is no linear term in that case.

4.3 The case $M = S^3 \setminus 7_2$.

The next example we studied that was important to the emerging picture was the complement of the knot 7_2 , which can be triangulated with 4 ideal tetrahedra. The results of our numerical experiments are shown in Figure 3. This example revealed a more complicated picture than we expected from the first few computations. In this case the function we fit to the experimental data is a combination of **several** trigonometric summands as well as a linear term:

$$0.1570\kappa + 0.8154\sqrt{\kappa} \cos\left(\text{Vol}_{\mathbb{H}}(S^3 \setminus 7_2)\kappa + \frac{\pi}{4}\right) + 0.8866\sqrt{\kappa} \cos\left(2.214\kappa + \frac{\pi}{4}\right). \quad (1)$$

Every example we studied to this point contained a trigonometric function with frequency given by the hyperbolic volume, but the example 7_2 presented us with a puzzle. What was this second frequency 2.214?

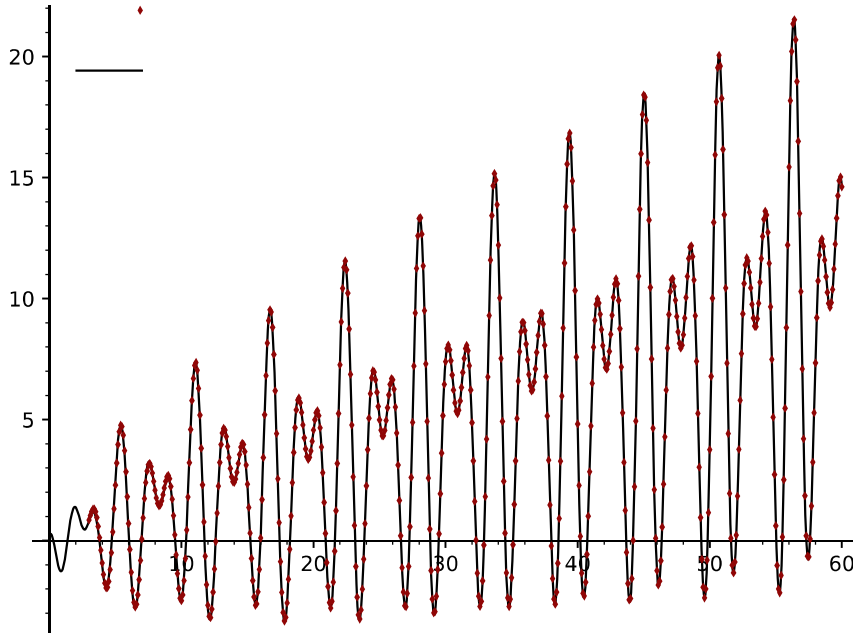


Figure 3: The case of the manifold $M = S^3 \setminus 7_2$. The curve shown fit to the computations is $0.1570\kappa + 0.8154\sqrt{\kappa} \cos(\text{Vol}_{\mathbb{H}}(S^3 \setminus 7_2)\kappa + \frac{\pi}{4}) + 0.8866\sqrt{\kappa} \cos(2.214\kappa + \frac{\pi}{4})$.

Considering these and other examples we computed, we were led to the following hypothesis.

First Hypothesis. The leading asymptotics of the value $I_{M, e^{-1/\kappa}}(1, 1)$ as $\kappa \rightarrow \infty$ are given by a sum of terms corresponding to boundary-parabolic $PSL(2, \mathbb{C})$ -representations of the fundamental group of M . If the representation is not real, then the frequency of the corresponding contribution is given by the volume associated to that representation.

Let us explain this hypothesis in terms of the example we just described, $M = S^3 \setminus 7_2$. The boundary-parabolic $PSL(2, \mathbb{C})$ -representations of an ideally-triangulated 3-manifold can be computed, for example by using Ptolemy co-ordinates [10]. The results have been tabulated into an online database by Matthias Goerner [9]. If we inspect the entry in that database for the complement of the knot 7_2 , we learn that this manifold has exactly 5 boundary parabolic $PSL(2, \mathbb{C})$ representations:

1. The representation corresponding to the complete hyperbolic structure, $\rho_{\text{geom.}}$. This representation has volume $\text{Vol}(\rho_{\text{geom.}}) = 3.3317$.
2. The complex conjugate of that representation: $\overline{\rho_{\text{geom.}}}$. This representation has volume $\text{Vol}(\overline{\rho_{\text{geom.}}}) = -3.3317$.
3. An additional complex boundary-parabolic representation ρ_1 with volume $\text{Vol}(\rho_1) = 2.2140$.
4. The complex conjugate of that representation $\overline{\rho_1}$ with volume $\text{Vol}(\overline{\rho_1}) = -2.2140$.

5. A **real** boundary-parabolic representation. By real is meant its image lies in the subgroup $PSL(2, \mathbb{R})$.

The important observation is that the first frequency we see in the computed asymptotics of the manifold $M = S^3 \setminus 7_2$ is, as expected, the hyperbolic volume of the manifold. But the second frequency we see, 2.214, is in fact the volume of the *second* complex boundary-parabolic $PSL(2, \mathbb{C})$ -representation.

The picture we are led to is the following. The first representation on the list (coming from the complete hyperbolic structure) should contribute a term of the general form $C\sqrt{\kappa}e^{i(\text{Vol}(\rho_{\text{geom.}})+\frac{\pi}{4})}$ for some real constant C . The complex conjugate of this representation (the second representation on the list) should contribute the complex conjugate of this term. Then the sum of two terms accounts for the piece

$$0.8154\sqrt{\kappa} \cos\left(\kappa \text{Vol}_{\mathbb{H}}(S^3 \setminus 7_2) + \frac{\pi}{4}\right)$$

in Equation 1.

Similarly, the other complex representation ρ_1 (the third representation on this list) should also contribute such a term $D\sqrt{\kappa}e^{i(\text{Vol}(\rho_1)+\frac{\pi}{4})}$ for some real constant D . And its complex conjugate representation (the fourth representation on this list) should contribute the complex conjugate of that term. The sum of these two terms should account for the following term from Equation 1:

$$0.8866\sqrt{\kappa} \cos\left(2.214\kappa + \frac{\pi}{4}\right).$$

Finally: the real boundary-parabolic representation (the fifth representation on the list) should contribute remaining the linear term:

$$0.1570\kappa.$$

4.4 The case $M = m011$.

There was one final refinement we needed to make in this story to exactly pin down which boundary-parabolic $PSL(2, \mathbb{C})$ representations should be contributing to the asymptotics for our conjecture. This refinement can be detected by examining the example of the manifold $m011$, which is not a knot complement.

When we examine the database entry for this manifold [9] we learn that there are 7 boundary-parabolic $PSL(2, \mathbb{C})$ -representations:

	Complex volume	Type	
1.	$2.7818 - 0.4968i$	\mathbb{C}	Conjugate of 1.
2.	$-2.7818 - 0.4968i$	\mathbb{C}	
3.	$0 + 0.6810i$	\mathbb{R}	
4.	$0 + 0.3127i$	\mathbb{R}	
5.	$0.9427 + 0.4597i$	\mathbb{C}	Conjugate of 5.
6.	$-0.9427 + 0.4597i$	\mathbb{C}	
7.	$0 + 0.7255i$	\mathbb{R}	

(2)

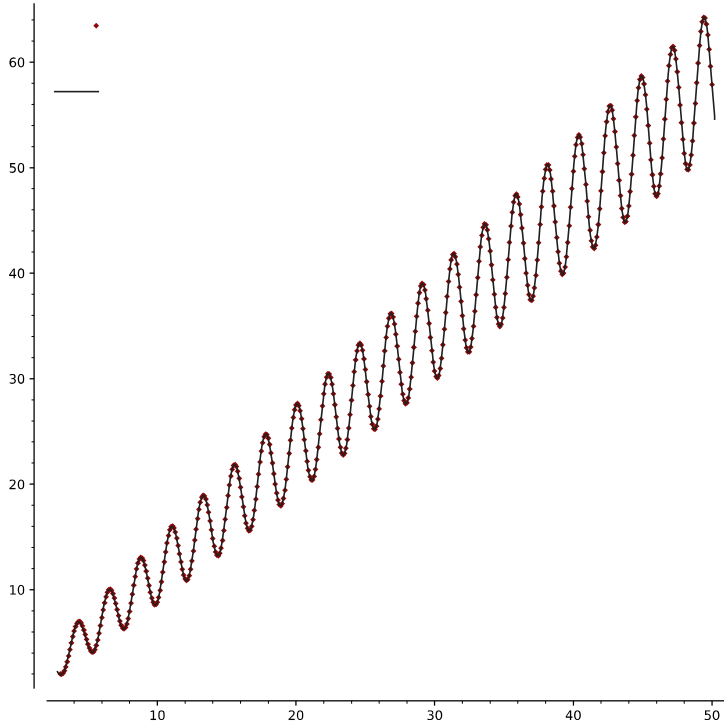


Figure 4: The case of the manifold $M = m011$. The curve shown fit to the computations is $1.1666\kappa + 0.9437\sqrt{\kappa} \cos(\kappa \text{Vol}_{\mathbb{H}}(m011) + \frac{\pi}{4})$.

The topological meaning of the division of this list into two groups is crucial and will be discussed shortly.

The results of our computation of this example are presented in Figure 4.

The important thing to note about this example is what does *not* appear. There is a complex conjugate pair of complex boundary-parabolic representations on the list (the ones with volume ± 0.9427) which apparently do not contribute a term to the asymptotic behaviour. Indeed, there does not seem to be a trigonometric component with frequency 0.9427.

The explanation for this is that there is an extra piece of topological information that can be derived from a boundary-parabolic representation $\rho : \pi_1(M) \rightarrow PSL(2, \mathbb{C})$. Each such representation determines a cohomology class $\Phi_0(\rho) \in H^2(M, \partial M; \mathbb{F}_2)$. The cohomology class $\Phi_0(\rho)$ is precisely the obstruction to lifting the boundary-parabolic representation ρ to a boundary-unipotent representation $\hat{\rho} : \pi_1(M) \rightarrow SL(2, \mathbb{C})$.

The two boxes we see in the table 2 show the partition of the set of boundary-parabolic representations according to this obstruction class.

This example m011 suggests that the asymptotics should have one contribution from each representation with a certain specified obstruction class.

Second, refined, version of the hypothesis. The leading asymptotics of the value $I_{M, e^{-1/\kappa}}(1, 1)$ as $\kappa \rightarrow \infty$ are given by a sum of terms corresponding to boundary-parabolic

$PSL(2, \mathbb{C})$ -representations of the fundamental group of M which have the same obstruction class to lifting to a boundary-unipotent $SL(2, \mathbb{C})$ -representation as the representation coming from the complete hyperbolic structure.

5 Our conjecture

Motivated by, and developed alongside these numerical investigations, we performed an asymptotic analysis of the Garoufalidis-Kashaev state integral to develop a precise conjecture for the asymptotic behaviour of the meromorphic state-integral of a hyperbolic 1-cusped manifold at this point $(1, 1)$. The key analytic tools we exploited were stationary-phase techniques. We also needed various other special analytic tools, especially to study the contributions from the real representations which required a separate analysis. These tools included some new asymptotic expansions of quantum dilogarithms. The full story is detailed in our article [1].

To finish the present article, we'll introduce our asymptotic expansion conjecture.

The starting point for the conjecture, as we discovered in our numerical investigations described earlier, is that the leading asymptotics should consist of a sum of contributions associated to the conjugacy classes of boundary-parabolic $PSL(2, \mathbb{C})$ representations satisfying the cohomological condition that their associated obstruction class is the same obstruction class as the representation coming from the geometric structure.

Next we have to detail what the corresponding contributions should be. There should be two types of contributions: the contributions associated to representations which are not real, and the contribution from those that are.

To outline the conjecture we introduce various notation:

- Let $\rho^{\text{geom}} : \pi_1(M) \rightarrow PSL(2, \mathbb{C})$ denote the boundary-parabolic representation (defined up to conjugation only) associated to the complete hyperbolic structure of finite volume.
- A representation $\rho : \pi_1(M) \rightarrow PSL(2, \mathbb{C})$ will be called a *real representation* if it can be conjugated to lie in the subgroup $PSL(2, \mathbb{R}) \subset PSL(2, \mathbb{C})$. Otherwise it will be called a *complex* representation.
- $\mathcal{X}^{\text{geom}}$ will denote the set of conjugacy classes of irreducible, boundary-parabolic representations $\rho : \pi_1(M) \rightarrow PSL(2, \mathbb{C})$ with the same obstruction class as ρ^{geom} .
- $\mathcal{X}_{\mathbb{R}}^{\text{geom}} \subset \mathcal{X}^{\text{geom}}$ denotes the subset consisting of real representations.

Our conjecture has the following general form:

$$I_{M, e^{-1/\kappa}}(1, 1) = \sum_{[\rho] \in \mathcal{X}_{\mathbb{R}}^{\text{geom}}} \mathcal{C}_{\mathbb{R}}([\rho], \kappa) + \sum_{[\rho] \in \mathcal{X}^{\text{geom}} \setminus \mathcal{X}_{\mathbb{R}}^{\text{geom}}} \mathcal{C}_{\mathbb{C}}([\rho], \kappa) + o(1), \quad \text{as } \kappa \rightarrow \infty. \quad (3)$$

Here $\mathcal{C}_{\mathbb{R}}([\rho], \kappa)$ denotes a contribution associated to a conjugacy class of real representation $[\rho]$, which we postulate to be a linear function of the parameter κ :

$$\mathcal{C}_{\mathbb{R}}([\rho], \kappa) = |H_1(\hat{M}; \mathbb{F}_2)| \cdot \mathcal{I}_{\text{MB}}(\rho) \kappa, \quad (4)$$

where \hat{M} denotes the 3-complex extending M which is obtained when the vertices of the ideal triangulation are retained, and $\mathcal{I}_{\text{MB}}(\rho)$ is a new invariant of (boundary-parabolic) $PSL(2, \mathbb{R})$ -representations of $\pi_1(M)$. This invariant can be formulated explicitly in terms of a certain multivariate contour integrals of Mellin–Barnes type [1]. This invariant is presented in more detail in the problems section of this conference’s proceedings.

The contributions coming from complex representations are denoted $\mathcal{C}_{\mathbb{C}}([\rho], \kappa)$. If ρ is such a representation and $\bar{\rho}$ is its complex conjugate representation, then we conjecture the two contributions will pair up in the following way:

$$\mathcal{C}_{\mathbb{C}}([\rho], \kappa) + \mathcal{C}_{\mathbb{C}}([\bar{\rho}], \kappa) = C_{\rho} \sqrt{\kappa} \cos \left(\kappa \text{Vol}(\rho) + \frac{\pi n_{\rho}}{4} \right), \quad (5)$$

where $C_{\rho} > 0$, $n_{\rho} \in \mathbb{Z}$, and $\text{Vol}(\rho) \in \mathbb{R}$ denotes the volume of the representation ρ . (See [10] for a discussion of this concept of volume associated to such a representation.)

Of particular interest is the prefix C_{ρ} . In [1] we prove it is exactly a simple normalization of the 1-loop invariant introduced by Garoufalidis and Dimofte [2].

6 Acknowledgement

The project received support through the AcRF Tier 1 grant RG 32/17 from the Singapore Ministry of Education. This article was prepared at the Research Institute for Mathematical Sciences at Kyoto University while the author was a guest of Tomotada Ohtsuki. The author thanks Tomotada Ohtsuki for this support.

References

- [1] Hodgson, C., Kriker, A., Siejakowski, R., *On the asymptotics of the meromorphic 3D-index*, arXiv:2109.05355.
- [2] Dimofte, T., Garoufalidis, S., *The quantum content of the gluing equations*, *Geometry & Topology* **17(3)** (2013) 1253–1315.
- [3] Tudor, D., Gaiotto, D., Gukov, S., *3-manifolds and 3D indices*, *Adv. in Theor. and Math. Physics* **17(5)** (2013) 975–1076.
- [4] Tudor, D., Gaiotto, D., Gukov, S., *Gauge theories labelled by 3-manifolds*, *Communications in Mathematical Physics* **325(2)** (2014) 367–419.
- [5] Garoufalidis, S., *The 3D index of an ideal triangulation and angle structures*, *Ramanujan Journal* **40(3)** (2016) 573–604.
- [6] Garoufalidis, S., Hodgson, C., Hoffman, N., Rubinstein, H., *The 3D-index and normal surfaces*, *Illinois Journal of Mathematics* **60(1)** (2016) 289–352.
- [7] Garoufalidis, S., Hodgson, C., Rubinstein, H., Segerman, H., *1-efficient triangulations and the index of a cusped hyperbolic 3-manifold*, *Geometry and Topology* **19(5)** (2015) 2619–2689.

- [8] Garoufalidis, S., Kashaev, R., *A meromorphic extension of the 3D index*, Res. Math. Sci. **6** (2019), Paper No. 8, 34 pp.
- [9] Goerner, M., The Ptolemy database. <http://ptolemy.unhyperbolic.org/>.
- [10] Garoufalidis, S., Thurston., D., Zickert, C., *The complex volume of $SL(n, \mathbb{C})$ -representations of 3-manifolds*, Duke Math. Journal **164** (2015) 11, 2099–2160.

School of Physical and Mathematical Sciences
Nanyang Technological University
21 Nanyang Link
Singapore 637371